

Subsurface Investigation within Quaternary Alluvium Formation Using Electrical Resistivity Imaging in Birnin Kebbi, Northwestern Nigeria

A. Adamu^{1*}, H. Sunusi²

¹Department of Applied Geophysics, Federal University, Birnin Kebbi, Nigeria; ²Department of Physics, Usmanu Danfodio University, Sokoto, Nigeria

ABSTRACT

2D Electrical Resistivity Imaging (ERI) was carried out with the aim of characterizing subsurface layers in order to delineate the alluvium cover within the quaternary formation in Birnin Kebbi and its environs. The objective of this paper is to demonstrate the applicability of the Electrical resistivity imaging (ERI) for mapping of subsurface system within the area of study in terms of layering and layer thickness. Five profiles were occupied in the study area. For each profile, two reels of cables were laid collinearly with 5 m intervals between the outermost electrodes. Each reel had 21 outermost electrodes. However, the two innermost electrodes of the two reels of cables were connected together, thus yielding effectively 42 electrodes and a special length of 200 m. The data obtained using ABEM Terrameter SAS 1000 with electrodes selector were processed using RES2DINV software. The results of this survey in correlation with borehole data revealed four distinct layers: the Lateritic clay (Topsoil) which is about 1.83 to 2.00 m and between 35 to 55 m thick having a resistivity ranging 63.4 Ω m - 91.7 Ω m, the second layer which is a lateritic layer, Sandy Clay (soft overburden) with apparent resistivity ranging from about 112.35 Ω m, to 582 Ω m, occurred at depth ranging from 0 to 19.4 m, the weathered basement is the third layer and has apparent resistivity range of between 582 Ω m to 712 Ω m, fresh basement with apparent resistivity values >700 Ω m occur at the base of this profile at depth of about 33.4 m at a lateral distance of 150 m along the profile. It can be concluded that the 2D Electrical Resistivity Imaging used in this research (i.e. ERI) are useful and powerful technique for mapping the subsurface and aquifer systems within the quaternary alluvial formation, and in other similar areas.

Keywords: 2D Electrical Resistivity Imaging (ERI); Quaternary alluvium; Wenner Configuration; ABEM Terrameter; Birnin Kebbi Metropolis

INTRODUCTION

The Quaternary alluvial deposit in Birnin Kebbi is lies within the agricultural region of farmland soil and it is characterized by a semi-arid climate with low average annual precipitation (around 350 mm/year) [1]. The rapid agricultural development in the area has caused a high increase in demand for water supply. Therefore, the drilling of wells has increased considerably in recent years—by the year 2015 the estimated number of wells was around 205 [2,3]. The monitoring of the groundwater level shows a decreasing trend of the water table, and probably the

main reason for this decline is due to the fact that groundwater extraction has equaled or exceeded the natural recharge during the last few years [4].

Electrical resistivity profiling methods are near surface geophysical techniques for engineering and environmental applications [5]. In the last few decades the development of multi-electrode arrays, automatized acquisition systems, and new inversion algorithms has renewed the interest in these methods. Electrical Resistivity Imaging (ERI) is one of the most commonly used geophysical methods for imaging subsurface features. This technique

Correspondence to: A. Adamu, Department of Applied Geophysics, Federal University Birnin Kebbi, Nigeria, E-mail: adamu.abubakar35@fubk.edu.ng

Received: February 22, 2021; **Accepted:** March 8, 2021; **Published:** March 15, 2021

Citation: Adamu A, Sunusi H (2021) Subsurface Investigation within Quaternary Alluvium Formation Using Electrical Resistivity Imaging in Birnin Kebbi, Northwestern Nigeria. J Geol Geophys. 10:493.

Copyright: © 2021 Adamu A, et al. This is an open-access article distributed under the terms of the Creative Commons Attribution License, which permits unrestricted use, distribution, and reproduction in any medium, provided the original author and source are credited.

estimates the distribution in resistivity of the ground, which can vary with water content and lithology. The resistivity distribution can be interpreted from a hydrogeological point of view [3]. In the ERI surveys, the measured quantity is called apparent resistivity (“ ρ_a ”), which is the equivalent, to resistivity for a homogeneous soil volume which yields the same potential value as the true model. In order to estimate the true resistivity distribution, an inverse numerical modeling (inversion) is used to create a model based on the apparent resistivity data [6]. The inversion adjusts a finite difference or finite element model in an iterative process [7-9] by comparing the measured apparent resistivity versus the calculated resistivity from the inverted model. The use of Electrical Resistivity Imaging (ERI) profiling, makes it possible to estimate the thickness, depth, and morphology of different units of the subsurface [10-12].

Worldwide, many electrical resistivity surveys have been applied in a wide range of geological studies [13], but there has not been any research that has used Electrical resistivity imaging (ERI) within the area of study, according to our knowledge. In order to fill in the gaps and demonstrate the applicability of indirect data retrieved from electrical resistivity profiling methods in alluvial deposits, a case study was carried out in this area. Generally Geophysics provides some of the required information to delineate those materials in the subsurface of the earth. Many Geophysical techniques are available which can be used to map and delineate the subsurface. In this work, electrical resistivity imaging (ERI) methods using Wenner configuration was employed in order to delineate and characterize the subsurface in terms of layering and layer thickness within the quaternary alluvium formation in Birnin Kebbi and its environs.

GENERAL GEOLOGY OF THE STUDY AREA

The geology of the area is predominantly a gentle undulating plain with an average elevation varying from 250 m to 400 m above sea level. The plain is occasionally interrupted by low mesas and other escarpment feature. Birnin Kebbi is part of the Sokoto Basin of the Nigeria sector of the larger Iullemeden Basin; the Iullemeden Basin itself is a broader sedimentary basin covering most part of Algeria, Niger Republic, Benin Republic, Mali, and Libya. The geology of Kebbi State is dominated by two formations Precambrian Basement complex in the South to southeast and young sedimentary rocks in the North. The basement complex region is composed of very old volcanic and metamorphic rocks such as granites, schist, gneisses, and quartzite consist of Gwandu, Illo and Rima group whose ages range from cretaceous to the Eocene (Figure 2). The Gwandu group consists of massive of clay interbedded with sandstone while Illo and Rima group consist of Pebbly grits, sandstones and clays, mudstones and siltstones respectively mineral that can be found in the state include quarts, Kaolin, photolytic bauxite, clay, potassium, silica sand, and salt [14]. The sediment dips gently and thickens gradually toward the northwest with maximum thicknesses attainable toward the border with Niger Republic (Figure 2). The study are was

chosen since they have geology record of thick alluvium (Figure 1).

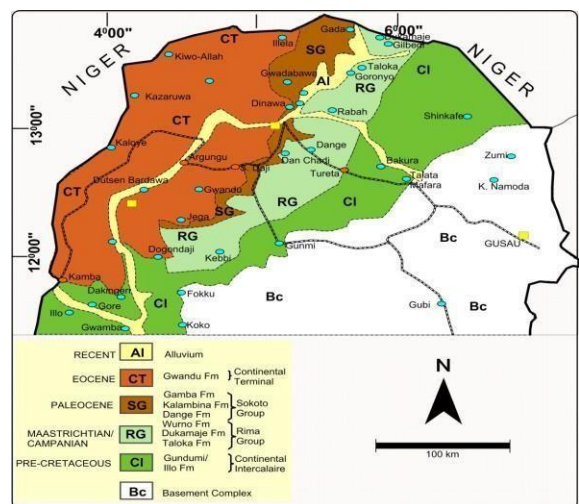


Figure 1: Generalized Geological Map of Sokoto.

LOCATION AND ACCESSIBILITY OF THE STUDY AREA

The study area is situated in Birnin Kebbi and its environs Kebbi State NW Nigeria sharing a boundary with Niger republic and also shares a southern border with Kangiwa L.G.A in Kebbi State Nigeria, located between latitude 12° 26'.008" N to 12° 29' 012" N and longitude 4° 9' 0" E to 4° 12'.0" E with mean altitude of about 256 m above sea level (Figure 1). The age indicated for the formation is early Eocene to Miocene (Figure 2). The area is central to most major towns and communities in the district and fades with agricultural irrigation farming (Figure 2).

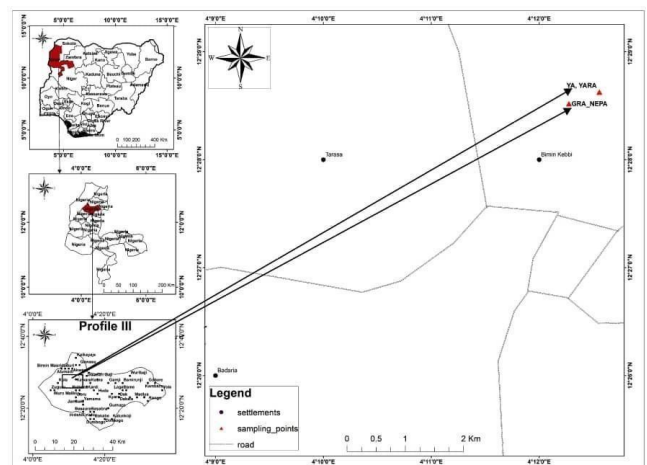


Figure 2: Location Map of the Study Area.

MATERIALS AND METHOD

Introduction

2D electrical resistivity Imaging (ERI) surveys were carried out within the quaternary alluvium of Gwandu formation in Birnin Kebbi. ABEM SAS 1000 Terrameter, smart cables and reels, 21 stainless steel electrodes and jumpers, global positioning system (GPS) was used for the surveys. For this survey Wenner array with 5m electrode spacing, 2 mA minimum and 20 mA maximum current was used based on the expected depth of penetration, beside it provide a good resolution. Wenner array is an arrangement in which the spacing is equal between the two electrodes across and measured the apparent resistivity. The raw data was processed and interpreted using RES2DINV software on an inexpensive microcomputer. Boring was performed on every survey line for correlation with the 2D ERI result.

2D electrical resistivity Imaging (ERI) is now mainly carried out with a multi-electrode resistivity meter system (Figure 3). Such surveys use a number (usually 25 to 100) of electrodes laid out in a straight line with a constant spacing. A computer-controlled system is then used to automatically select the active electrodes for each measure [15] (Figure 3).

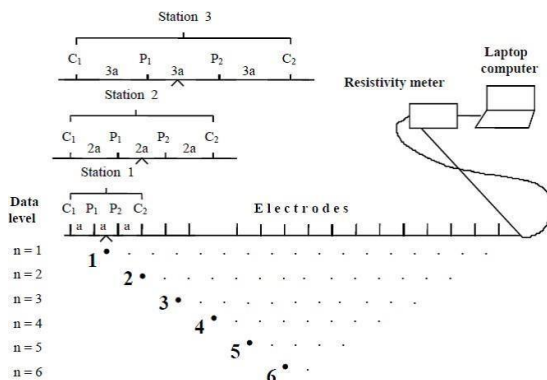


Figure 3: The arrangement of electrodes for a 2D electrical resistivity survey and the sequence of measurements used to build up a pseudo section.

Field procedure and data collection

A total of five established profiles of ERI surveys were measured within the Quaternary alluvial cover. All data were measured using ABEM Terrameter SAS 1000 equipment. Stainless steel electrodes and four electrode cables with 21 outermost each was used. The survey lines are designed in such a way to fulfill study objectives of the five established profiles (Figure 4).The maximum separation between electrodes was 5 m, providing a total spread length of 100 m between the outermost electrodes. The Wenner electrode array configuration was used; this array has proved to be more suitable for resistivity profiling data acquisition providing a significant increase in the Vertical and Horizontal changes of data points [16-18]. Elevations and coordinates of the electrodes were collected with a GPS and a Digital Elevation Model with a spatial resolution of 20 m x 20 m; the topography was included in the files before the inversion [12]. The selection of the ERI locations was predominately planned according to the

availability of areas free of obstacles such as houses, fences, crops, and paved roads; another problem confronted was getting the permission within the agricultural farm land owners to perform the surveys in their lands (Figure 4). When conditions allowed, the roll-along technique was applied for getting continuous profiles (Figure 4).

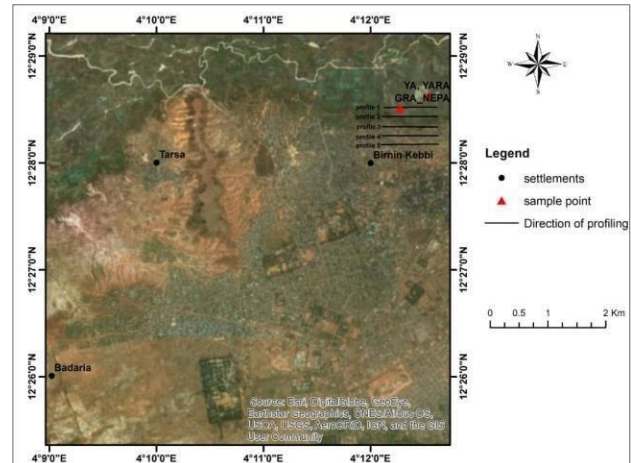


Figure 4: Established Profiles on Google Earth map of the Study Area.

RESULTS

Data processing

The raw field data were processed using RES2DINV [19]. This is a computer program that automatically determines a Two-dimensional (2D) resistivity model for the subsurface for the data obtained from electrical resistivity survey. It is a window based program.

The forward problem is solved through a finite difference algorithm, whose main features are a versatile user-defined discretization of the domain and a new approach to the solution of the inverse Fourier transform. The forward modeling subroutine is used to calculate the apparent resistivity values. The inverse procedure is based on an iterative smoothness-constrained least-squares algorithm. This computer program uses smoothness constrained non-linear least-squares optimization inversion technique to convert measured apparent resistivity values to true resistivity values and plot them in cross-sections.

The inversion process removes geometrical effects from the pseudo-section and produces an image of true depth and true formation resistivity. One advantage of this method is that the damping factor and flatness filter can be adjusted to suit different types of data. The program creates a resistivity cross-section, calculates the apparent resistivities for that cross-section, and compares the calculated apparent resistivities to the measured apparent resistivities. The iteration continues until a combined smoothness constrained objective function is minimized. The depth of investigation cannot be determined by simple calculations and it depends on the acquisition geometry, the conductivity structures and data errors [20].

Interpretation technique

Interpreting the resistivity data consists of two steps: a physical interpretation of the measured data, resulting in a physical model (geo-electric model), and a geological interpretation of the resulting physical parameters [14]. The large-scale data were processed with the state-of-the-art interpretation technique, called the 2D smoothed damped least squares inversion algorithm. The results in 2D images obtained based on the 2D inversion of field data, were interpreted with borehole information as guide to determine the lithology of the area. Contours tend to follow horizontal or gently sloping boundaries between strata of different resistivity, though steep contacts are much smoothed. Steep boundaries, provided they show a strong resistivity contrast, can be identified using some of the gradient measure. Contour peaks and troughs are correctly positioned relative to the subsurface features giving rise to them, and some estimate of depths at which boundaries occur may be made [21].

Qualitatively speaking, subsurface structure may be quite obvious though this is by no means always so, if there are marked departures from ‘two dimensionality,’ the contour pattern may be affected by resistivity contrasts close to, but outside the plane of the section. Such effects can lead to serious errors both at the qualitative and quantitative stages of interpretation. Also faulting can be difficult to detect due to the smoothing effect of the Wenner array [22]. Even if the acquisition of a data set is straightforward due to the improvements in resistivity devices, the interpretation involves many factors and can be difficult when some parameters in the inversion procedure are neglected. Such parameters include the stability, robustness and uniqueness of the inversion algorithm [18].

Geologic Section from Borehole Data

Boreholes log data are often used to correlate results obtained from geophysical electrical drilling as these surveys are indirect. This is often done by correlating apparent resistivity obtained in an area with the lithological information obtained in the area. Boreholes are necessary and reliable sources of primary data and Electrical Resistivity Imaging (ERI) interpretations provide secondary information. Although borehole data provide a good sample for a six-inch diameter vertical cylindrical volume, it can be a poor representation of the several square meters surrounding the borehole. The 2D inversion results of the survey were correlated with Borehole log taken within the study area (Figure 5).





Depth (m)	Lithology	Drillers Description	Geological Interpretation
0 - 20		Sedimentary Rock	Soft Overburden
20 - 35		Granite	Weathered/ Fresh Basement
35 - 40		Gap	Fractured Basement
40 - 50		Granite	Fresh Basement

Figure 5: Geological Correlation of Drillers Log with Data from this Study.

Interpretation of Results

Profile 1

Figure 6 shows the inverse resistivity model of the study area along profile 1, runs from East-West direction displays three distinct layers within a root mean square error of 10.7%, with resistivity values <100 Ωm which indicate an alluvium soft overburden (Figure 5). Drilling records within the study area shows the lithology description and Geological interpretation. The profile consists of three layers; overburden layer, weathered and fresh layer. The result show lateritic clay and Clay with resistivity values of (26 Ωm-160 Ωm), while Sandy Clay with (50 Ωm-100 Ωm) and Saturated Sandy Clay (170 Ωm-300 Ωm). This lateritic layer extends at a lateral distance of 5 m-18.0 m and a depth of 0-6.4 m. The weathered/lateritic covered a lateral distance of 10 m-16.5 m and a depth of 6.5 m-24 m. The fresh basement layer covered a lateral distance of 50 m-165 m and a depth of 25 m-33.8 m (Figure 6).

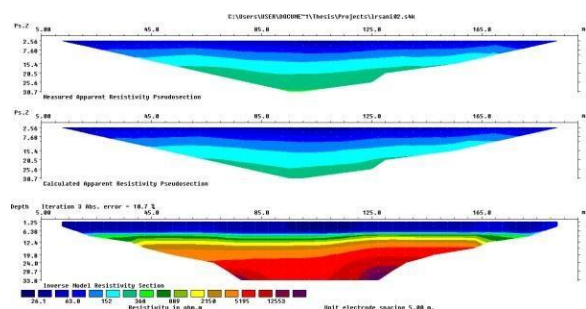


Figure 6: Results of 2D inversion of Wenner array along Profile 1.

Profile 2

The traverse was run from East-West within the study area. Four distinct layers were displayed by the inverse resistivity model (Figure 7). These are: lateritic layer including topsoil, lateritic clay, Clay weathered region and fresh basement. The lateritic layer which includes the topsoil has apparent resistivity ranges from less than

(83.1 Ωm –400.5 Ωm). Laterally; this layer extends from the beginning of the profile to a distance of 18.0 m along the traverse. It reaches up to depths of about 20.65m. The first lateritic layer is intercalated with lateritic clays which have lower apparent resistivity ranging from (23.8 Ωm –83.1 Ωm). The third layer along this profile is the weathered basement with apparent resistivity range of (400.5–1206 Ωm). It occurs at depths of between (14.5–27.0 Ωm). It overlies the fourth layer which is the fresh basement which has apparent resistivity values varying greater than 5799 Ωm (Figure 7).

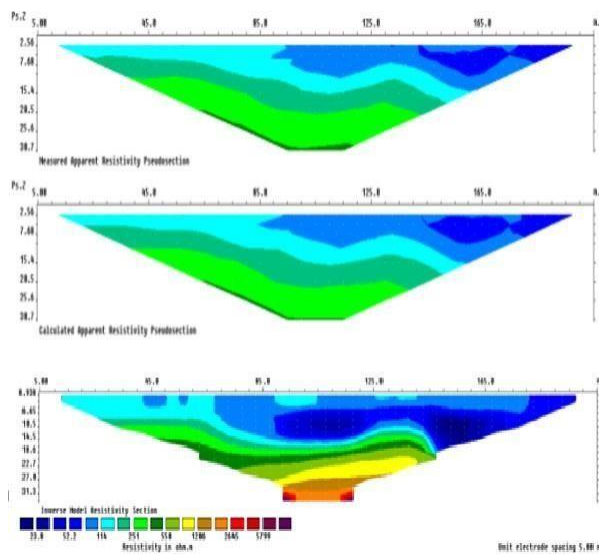


Figure 7: Results of 2D inversion of Wenner Array along Profile 1.

Profile 3

The profile was measured over a huge sand deposit beside a stream where contaminated wastes are disposed of. In the pseudo section, a region of averagely low resistivity indicate top-layer sand deposit saturated with conductive fluid dissipated from a stream river channel to a depth of 6 meters throughout the lateral extent. Below this relatively low resistivity layer 53.4 Ωm –100.65 Ωm , is a stretch of lateritic deposit clustered with deeply buried river sand. The lateritic bed is largely non-porous to the conducting fluid saturating the upper lying porous formation. Sand varies in particle size and in compaction and some types of sand have low bearing capacity.

Profile 4

The trend from East-West along the quaternary alluvium close to Takalau irrigation agricultural farm land along profile 4. Inverse resistivity model sections of this profile also reveal four separate layers (Figure 7). The first been the lateritic clay, Sandy Clay, Coastal Sand, having the lowest apparent resistivity ranging from less than 65.2 Ωm –129 Ωm , 129 Ωm –377 Ωm and 377 Ωm –745 Ωm . It occurs at horizontal distances of 1.75 m–3.0 m and 8.5 m–17.0 m from the beginning of the profile, and occurs at depths ranging from 0–6.76 m. Depth range of occurrence of layer is from 0–17.3 m. The fresh basement which underlies the weathered basement with apparent resistivity values obtained for this layer ranges from 745

Ωm –1405 Ωm at depths of about 10.08 m–31.3 m and beyond.

Profile 5

The profile trends SW-NE and is the second of the diagonal profiles carried out in this work. It is the only profile that reveals five (5) distinct layers. These are: lateritic clay, lateritic layer, weathered basement, fresh basement and fractured basement respectively. The lateritic clay forms the first layer with apparent resistivity range of 55.8 Ωm – 107.9 Ωm . Its occurrence is at a lateral distance of about 105 m, to the end of the profile. Maximum depth reached by this layer is about 6.76 m. Lateritic layer which the second is observed stratum has apparent resistivity ranging from 107.9 Ωm –393.5 Ωm . The layer is exposed at the surface at lateral distances of 0–35 m and 55 – 105 m respectively. Depth found of this layer is from 0–10.08 m (maximum depth occurring at a lateral distance of 30 m from profile start). The third layer along this profile is the weathered/lateritic region with apparent resistivity values ranging from 393.5 Ωm –735 Ωm . The layer is partly exposed a lateral distance of 35–50m along the profile and reaches depths of about 13.4 m. The fresh basement forms the fourth layer and has apparent resistivity ranges of 735 Ωm –1132 Ωm . It also outcrops/ridges at the surface of a horizontal distance of between 50 m–55 m along the profile. It reaches depths of 36.9 m and beyond. The fifth and final layer is the fractured zones which occur beneath the fresh region at a lateral distance of 85m along the profile and a depth of 31.3 m. The apparent resistivity range of this layer obtained from the inverse resistivity model ranges from 201 Ωm –735 Ωm [23].

Correlation of 2D Resistivity Section with BoreholeLog

The 2D resistivity tomography has revealed the varying depth of soil materials along each transverse and also their resistivity values at each layer. The borehole log revealed the depth range of the weathered/lateritic region and fresh region to be between 0–5.0 m, 5.0 m–10.0 m, 10.0 m–15.0 m, 20.0 m–38.0 m and >40 m respectively. This range of depth agrees with the 2D ERT depths of profile one, three and six with resistivity range of 400 Ωm to 550 Ωm for weathered region and a range of 1000 Ωm to 1200 Ωm for the fresh basement [24].

Shows the correlation of the borehole log with the 2D inversion of the five established profiles. In addition, the 2D electrical resistivity imaging has shown the lateral extent of lithological formation of the subsurface, of which the borehole log could not. This clearly shows the need for the integration of resistivity tomography into various subsurface investigations within quaternary formation [25].

CONCLUSION

A geophysical investigation has been carried out within the Quaternary alluvium formation at Birnin Kebbi and its Environs, NW Nigeria. Five 2D electrical resistivity profiles were carried out in order to delineate the subsurface structures within the quaternary formation and its environs. Result of the geophysical survey indicates that the topsoil is within the depth range of 0 to 20 m and it is reflective of varying resistivity which

indicates materials suspected to be decomposed organic and vegetal remains, and exotic materials used in sand filling of the area. The second geoelectric pseudo layer is composed of lateritic clay material within the depth range of 7.0 m to 16.0 m and resistivity range of 65.2 Ω m to 129 Ω m. The lateritic clay material is with varying thicknesses and poor geotechnical properties which make it inimical to the foundation of engineering structures. The third geoelectric layer is composed of weathered basement having thickness range of 30.0 m to 52.5 m and resistivity value range of 129 Ω m-377 Ω m. The fourth geoelectric layer is composed of fresh basement within the depth range of 15 to 66 m and resistivity range of 90 to 180 Ω m. Sand material (>200 m) is prevalent towards the East-West of the study area which represents the competent layer for agricultural farming and the hydrogeologic unit with very good quality water within the study area. The result of the 2D electrical resistivity has been correlated well with that of the borehole log. The 2D resistivity survey has provided valuable information on the lateral and vertical variation of the layer competent for subsurface investigation within quaternary formation.

REFERENCES

- Hassani K, Shio MT, Martel C, Faubert D, Olivier M. Absence of metalloprotease GP63 alters the protein content of leishmania exosomes. *PLoS One*. 2014;9(4).
- Ramírez-Flores CJ, Cruz-Mirón R, Mondragón-Castelán ME, González-Pozos S, Ríos-Castro E, Mondragón-Flores R. Proteomic and structural characterization of self-assembled vesicles from excretion/secretion products of *Toxoplasma gondii*. *J Proteomics*. 2019;208:103-490.
- Mercier C, Dubremetz J-F, Rauscher B, Lecordier L, Sibley LD, Cesbron-Delauw M-F. Biogenesis of nanotubular network in *Toxoplasma* parasitophorous vacuole induced by parasite proteins. *Mol Biol Cell*. 2002;13(7):2397-2409.
- Ramírez-Flores CJ, Cruz-Mirón R, Arroyo R, Mondragón-Castelán ME, Nopal-Guerrero T, González-Pozos S, et al. Characterization of metalloproteases and serine proteases of *Toxoplasma gondii* tachyzoites and their effect on epithelial cells. *Parasitol Res*. 2019;118(1):289-306.
- Kalluri R, LeBleu VS. The biology, function, and biomedical applications of exosomes. *Science*. 2020;367(6478).
- Bebelmann MP, Smit MJ, Pegtel DM, Baglio SR. Biogenesis and function of extracellular vesicles in cancer. *Pharmacol Ther* [Internet]. 2018;188:1-11.
- Quek C, Hill AF. The role of extracellular vesicles in neurodegenerative diseases. *Biochem Biophys Res Commun*. 2017;483(4):1178-1186.
- Nazri HM, Imran M, Fischer R, Heilig R, Manek S, Dragovic RA, et al. Characterization of exosomes in peritoneal fluid of endometriosis patients. *Fertil Steril*. 2020;113(2):364-373.
- Boukouris S, Mathivanan S. Exosomes in bodily fluids are a highly stable resource of disease biomarkers proteomics. *Clin Appl*. 2015;9(4):358-367.
- Sancho-Alberio M, Navascués N, Mendoza G, Sebastián V, J Geol Geophys, Vol.10 Iss.2 No:493
- In general, in the study area for resistivity values lower than 100 Ω m the material is expected to have a high content of clay. Values of resistivity greater than 100 Ω m were linked to coarse grained material. These coarse materials ranged from boulders to sand; the grain size and resistivity decreased with depth. The 2D Electrical resistivity imaging used in this investigation demonstrated the applicability and efficiency in defining the layering and thicknesses of the different geological units within the quaternary alluvial deposits. It can be concluded that the 2D Electrical Resistivity Imaging used in this research (i.e. ERI) are useful and powerful technique for mapping the subsurface and aquifer systems within the quaternary alluvial formation, and in other similar areas.

Recommendation

Based on the result of this research work, the following is recommended:

A 2D seismic refraction survey should be conducted in the study area to further complement the results.

A Ground characterization of magnetic and radiometric should be conducted also within the study area.

Arruebo M, Martín-Duque P, et al. Exosome origin determines cell targeting and the transfer of therapeutic nanoparticles towards target cells. *J Nano biotechnology*. 2019;17(1):16.

- Deathage BL, Cookson BT. Membrane Vesicle Release in Bacteria, Eukaryotes, and Archaea: a Conserved yet Underappreciated Aspect of Microbial Life. Andrews-Polymenis HL, editor. *Infect Immun*. 2012;80(6):1948-1957.
- Schorey JS, Cheng Y, Singh PP, Smith VL. Exosomes and other extracellular vesicles in host-pathogen interactions. *EMBO Rep* [Internet]. 2015;16(1):24-43.
- Ratajczak J, Wysoczynski M, Hayek F, Janowska-Wieczorek A, Ratajczak MZ. Membrane-derived microvesicles: Important and underappreciated mediators of cell-to-cell communication. *Leukemia*. 2006;20(9):1487-495.
- Quesenberry PJ, Aliotta J, Deregibus MC, Camussi G. Role of extracellular RNA-carrying vesicles in cell differentiation and reprogramming. *Stem Cell Res Ther*. 2015;6(1):1-10.
- Tao SC, Guo SC. Role of extracellular vesicles in tumour microenvironment. *Cell Commun Signal*. 2020;18(1):1-24.
- Dai J, Su Y, Zhong S, Cong L, Liu B, Yang J, et al. Exosomes: key players in cancer and potential therapeutic strategy. *Signal Transduct Target Ther*. 2020;5(1).
- Huotari J, Helenius A. Endosome maturation. *EMBO J*. 2011;30(17):3481-3500.
- Johnstone RM, Adam M, Hammond JR, Orr L, Turbide C. Vesicle formation during reticulocyte maturation. Association of plasma membrane activities with released vesicles (exosomes). *J Biol Chem*. 1987;262(19):9412-9420.
- Rashed MH, Bayraktar E, Helal GK, Abd-Ellah MF, Amero

Adamu A, et al.

- P, Chavez-Reyes A, et al. Exosomes: From garbage bins to promising therapeutic targets. *Int J Mol Sci.* 2017;18(3).
20. Silva VO, Maia MM, Torrecilhas AC, Taniwaki NN, Namiyama GM, Oliveira KC, et al. Extracellular vesicles isolated from *Toxoplasma gondii* induce host immune response. *Parasite Immunol.* 2018;40(9): 1-11.
21. Li Y, Liu Y, Xiu F, Wang J, Cong H, He S, et al. Characterization of exosomes derived from *Toxoplasma gondii* and their functions in modulating immune responses. *Int J Nanomedicine.* 2018;19(13):467-477.
22. Wowk PF, Zardo ML, Miot HT, Goldenberg S, Carvalho PC, Mörking PA. Proteomic profiling of extracellular vesicles secreted from *Toxoplasma gondii*. *Proteomics.* 2017;17:15-16.
- OPEN ACCESS** Freely available online
23. Li Y, Xiu F, Mou Z, Xue Z, Du H, Zhou C, et al. Exosomes derived from *Toxoplasma gondii* stimulate an inflammatory response through JNK signaling pathway. *Nanomedicine (Lond).* 2018;13(10):1157-1168.
24. Kim MJ, Jung BK, Cho J, Song H, Pyo KH, Lee JM, et al. Exosomes secreted by *Toxoplasma gondii*-infected L6 cells: Their effects on host cell proliferation and cell cycle changes. *Korean J Parasitol.* 2016;54(2): 147-154.
25. Jung BK, Kim E Do, Song H, Chai JY, Seo KY. Immunogenicity of exosomes from dendritic cells stimulated with *Toxoplasma gondii* lysates in ocularly immunized mice. *Korean J Parasitol.* 2020;58(2): 185-189.